arXiv:2306.02124v1 [cond-mat.quant-gas] 3 Jun 2023

The mixing-spacetime symmetry in the Floquet-Bloch band theory

Pei Wang[1]

[1]*Department of Physics, Zhejiang Normal University, Jinhua 321004, China*

(Dated: June 6, 2023)

We discover a class of spacetime symmetries unique to time-periodic systems, which we term "mixing symmetry" due to its combination of space and time coordinates in the symmetry transformation. We systematically enumerate the symmetry groups, and classify the corresponding Floquet-Bloch band theories by utilizing the winding number of quasi-energy. Moreover, we provide a comprehensive scheme for the experimental realization of these symmetries. The particle propagator exhibits an intriguing pattern that remains invariant even under transformations mixing space and time coordinates. We anticipate that this distinct feature can be observed in current cold atom experiments.

Introduction.— The study of Floquet-Bloch bands has emerged as a central topic in the field of nonequilibrium driven many-body dynamics [1–5]. Recent advancements in precise control and probing techniques have allowed for the realization of Floquet-Bloch bands in diverse platforms, including photonic waveguides [6], solid materials [7], and cold atom systems [8]. By employing periodic driving, these systems offer a unique opportunity to explore models that are challenging to realize in static setups [9–12]. Moreover, periodic driving enables the emergence of new states of matter that lack a static analog, leading to captivating phenomena in condensed matter physics, such as symmetry breaking [13–15], localization [16–18], and topological effects [2–5, 19].

Symmetry plays a fundamental role in the study of band theory, exerting profound effects on various aspects of band structures. Spatial symmetries such as rotation, mirror reflection, and space inversion have long been recognized for their ability to protect band crossings or generate degeneracies [20]. Time reversal, particle-hole, and chiral symmetry have been utilized in the renowned tenfold classification of insulators and superconductors [21]. This classification has been applied to provide a periodic table for the topological phases [22, 23], and more recently, it has been extended to the topological classification of Floquet-Bloch bands [24–27]. Moreover, researchers have recognized the critical interplay between space group symmetries and topology, culminating in the comprehensive topological classification of band structures for all 230 crystal symmetry groups [28–30]. Notably, in the realm of Floquet systems, the presence of intertwined spatial and temporal translations, including nonsymmorphic symmetries such as glide time-reversal or time glide reflection, can preserve spectral degeneracy and give rise to novel out-of-equilibrium phases [31–34].

But previous studies have overlooked a class of symmetries that is unique to time periodic systems and absent in static ones. These symmetries are referred to as mixing symmetries in this paper. Let us consider the coordinates in 1+1-dimensional spacetime as (t, x). A linear coordinate transformation can be represented as $(t', x')^T = A\,(t, x)^T$. If the matrix A contains non-zero off-diagonal elements, it is called a mixing transformation because it combines the space and time coordinates. One well-known example of a mixing symmetry is the Lorentz symmetry, which holds significant importance in quantum field theory. In the context of condensed matter physics, the Schrödinger equation treats space and time differently, making continuous mixing symmetry impossible. Nevertheless, this does not rule out the possibility of discrete mixing symmetries [35, 36]. Recently, it has been discovered that the spacetime crystals that exhibit a discrete Lorentz symmetry can be realized in ultracold atomic gases confined to an optical lattice [37, 38]. But the models are constructed on finite-sized lattices and do not exhibit continuous Floquet-Bloch bands in the thermodynamic limit.

In this paper, we present the first evidence of the existence of continuous Floquet-Bloch band theory that incorporates mixing symmetry. We thoroughly identify and classify the mixing groups in 1+1 dimensions. The resulting Floquet-Bloch theories are categorized based on both symmetry groups and the winding number of quasi-energy in the Brillouin zone (see Tab. I for a summary). Unlike previously studied symmetries, the operator of mixing symmetry does not commute or anti-commute with the Hamiltonian. Therefore, we rely on group representation theory for constructing models. The band theory with mixing symmetry exhibits a quasi-energy-momentum relation that remains invariant under mixing transformations. Consequently, the particle propagator in real spacetime exhibits invariance when the spacetime coordinates undergo the transformation A, which is a distinctive characteristic of mixing symmetry.

We discuss the possible realization of mixing symmetry in cold atoms on an optical lattice. The precise control achieved at the single-site level in experiments allows for programmable Hamiltonians with locally adjustable potential energies on each lattice site, facilitated by microelectromechanical systems mirrors [39, 40]. We show that the Floquet-Bloch band with mixing symmetry can be implemented using a quadratic quantum Fourier transform (QQFT) protocol [38] on a driven optical lattice that features only onsite potential and nearest-neighbor hopping. The mixing symmetry can be observed by locating a Bose-Einstein condensate on the lattice and monitoring the atom density.

Method.— When studying a quantum model, the usual approach involves writing down the Hamiltonian in real spacetime and then extracting the underlying symmetry from it.

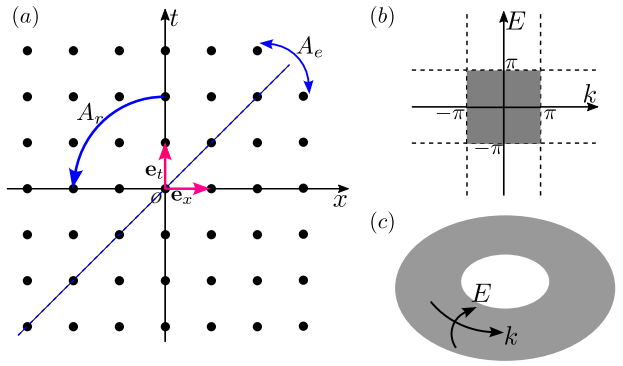


FIG. 1. (a) Schematic diagram of a spacetime crystal. The primitive vectors $\mathbf{e}_t$ and $\mathbf{e}_x$ define the unit cell. The mixing symmetry transformations, A_e and A_r, correspond to the exchange and rotation operations, respectively. (b) and (c) depict the Floquet-Bloch-Brillouin zone and its topological equivalence.

However, our objective is to construct a model with specific symmetry. We begin by providing a complete list of the mixing symmetry groups. Next, we establish the unitary representation of each group within the quasi-momentum-energy space. In this representation, the symmetry manifests as a constraint on the dispersion relation (DR), which is the function $E(k)$ describing the quasi-energy E as a function of quasi-momentum k. For continuous Floquet-Bloch bands, we discover a fundamental equation governing the topology of the DR, which serves as a basis for band classification. By finding an $E(k)$ that satisfies both the symmetry and topology conditions, we obtain the Floquet Hamiltonian $\hat{H}_F$. Finally, we demonstrate how to realize $\hat{H}_F$ using a time-periodic Hamiltonian $\hat{H}(t)$ with locality in real spacetime. Our approach is inspired by the principles of quantum field theory, which relies on the unitary representation of the Poincaré group [42].

Mixing groups.— We are considering a 1+1-dimensional spacetime where spatial rotation or mirror reflection is absent, allowing us to concentrate on the study of mixing symmetry.

	A	$\bar{A}$	Bands	Winding of DR
$\mathcal{P}_2$	$\begin{pmatrix} a & b \\ c & -a \end{pmatrix}$	$-A$	singlet	$w = \frac{-a-1}{b}$ or $\frac{1-a}{b}$
			doublet	$w_1 = w_2 = \frac{-a-1}{b}$ or $\frac{1-a}{b}$
$\mathcal{P}_4$	$\begin{pmatrix} a & b \\ c & -a \end{pmatrix}$	A	doublet	$w_1 = \frac{1-a}{b}$, $w_2 = \frac{-a-1}{b}$
			quadruplet	$w_1 = w_3 = \frac{1-a}{b}$, $w_2 = w_4 = \frac{-a-1}{b}$

TABLE I. Classification of Floquet-Bloch bands with mixing symmetry. A represents the coordinate transformation with $bc = -a^2 \pm 1$ for the symmetry classes $\mathcal{P}_2$ and $\mathcal{P}_4$, respectively, while $\bar{A}$ corresponds to the transformation in the k-E space. The bands are categorized as singlets, doublets, and quadruplets based on their mapping under $\bar{A}$. The winding number, denoted as w, distinguishes the winding properties of different bands.

There are two noncollinear translational vectors. Without loss of generality, we assign one vector ($\mathbf{e}_x$) to the spatial direction (x axis), and the other vector ($\mathbf{e}_t$) to the temporal direction (t axis), as shown in Fig. 1. This choice can always be made by employing a coordinate transformation that rotates $\mathbf{e}_t$ and $\mathbf{e}_x$ into the t and x axes, respectively. It is important to note that we exclusively consider symmorphic groups in this paper. For nonsymmorphic groups, nonsymmorphic symmetries may become significant when $\mathbf{e}_t$ and $\mathbf{e}_x$ are not orthogonal to each other [32]. To simplify the representation, we choose the lattice constants as the units of time and length, resulting in $\mathbf{e}_t = (1, 0)$ and $\mathbf{e}_x = (0, 1)$.

Suppose that the 2-by-2 matrix A represents a mixing transformation. In this study, we focus on cyclic transformations, which are the ones that satisfy $A^M = 1$ for some positive integer M (called the order). By imposing the cyclic condition, we significantly reduce the number of symmetry groups, enabling us to exhaustively examine their representations. An arbitrary symmetry transformation can be expressed as a combination of A and translation. We denote this combined transformation as $P(j, m, n)$, which acts on the coordinates as follows:

$$\begin{pmatrix} t' \\ x' \end{pmatrix} = P(j,m,n) \begin{pmatrix} t \\ x \end{pmatrix} = A^j \begin{pmatrix} t \\ x \end{pmatrix} + \begin{pmatrix} m \\ n \end{pmatrix}, \tag{1}$$

where j, m and n are integers. $P(j, m, n)$ denotes j times of mixing transformation followed by a translation of m units in time and n units in space. A symmetry group is a set of Ps that meet the group axioms. The closure under multiplication requires that the spacetime lattice $\left\{(m, n)^T \,|m, n \in \mathbb{Z}\right\}$ must keep invariant under A. Together with the existence of inverse element, we infer that the order of A can only be 2, 3, 4 or 6 [41]. The symmetry group can be expressed as

$$\mathcal{P} = \{P(j,m,n)\,|j = 0, 1, \cdots, M-1; \;\; m, n \in \mathbb{Z}\} \tag{2}$$

with $M = 2, 3, 4$ or 6. For given M, the group $\mathcal{P}_M$ is uniquely determined by A. The possible As in $\mathcal{P}_2, \mathcal{P}_3, \mathcal{P}_4$ or $\mathcal{P}_6$ are given in the supplementary materials.

A few examples can help us understand the mixing group. The form of A in $\mathcal{P}_2$ or $\mathcal{P}_4$ is shown in Tab. I, where a, b, c are integers satisfying $bc = -a^2 \pm 1$, respectively. If $a = 0$ and $b = c = 1$, then A is the exchange of t and x (dubbed A_e) and belongs to $\mathcal{P}_2$. If $a = 0, b = 1$ and $c = -1$, then A represents a rotation in the t-x plane by 90° (dubbed A_r) and belongs to $\mathcal{P}_4$. Figure 1a schematically illustrates the operations of A_e and A_r. The transformation A conserves the area of the parallelogram formed by two noncollinear vectors, because $\det(A) = \pm 1$. But A does not necessarily conserve the Euclidean length of a vector (e.g., consider the case $a = 2, b = -3$ and $c = 1$). Therefore, A can be not only rotation, reflection or inversion in the t-x plane, but also nonorthogonal transformations. Notice that A is distinguished from the discrete Lorentz transformation [35], as the latter does not have a finite order.

Floquet-Bloch band theory.— Each quantum theory is a unitary representation of its corresponding symmetry group. In our case, we aim to construct the unitary representations

of $\mathcal{P}_M$, and we follow a similar approach as described in Ref. [37]. To denote the unitary operator of $P(j,m,n)$, we use $\hat{U}(j,m,n)$, which follows the same multiplication rule as P. The translation operators $\hat{U}(0,m,n)$ commute with each other and share common eigenstates. In the Floquet-Bloch band theory, the eigenstates of translations are typically represented as $|k,\alpha\rangle$, where $k \in [-\pi,\pi)$ denotes the quasi-momentum, α is the band index, and the corresponding quasi-energy is denoted as $E_\alpha(k)$ with $E_\alpha(k) \in [-\pi,\pi)$. When the operator $\hat{U}(0,m,n)$ acts on $|k,\alpha\rangle$, it results in $e^{iE_\alpha(k)m-ikn}|k,\alpha\rangle$. The pair $(k,E_\alpha(k))$ represents a point in the Floquet-Bloch-Brillouin zone (FBBZ), which is topologically equivalent to a torus (see Fig. 1b,c). The DR of each continuous Floquet-Bloch band, i.e., the set of $(k,E_\alpha(k))$ points, forms a loop on the torus.

Since any element in $\mathcal{P}_M$ can be factorized into $P(j,m,n) = P(0,m,n)P(j,0,0)$, the representation of $\mathcal{P}_M$ can be determined by examining the action of the mixing transformation operator $\hat{U}(j,0,0)$ on the basis states $|k,\alpha\rangle$. Note that the single-particle Hilbert space is spanned by $|k,\alpha\rangle$. To determine the representation, it is sufficient to investigate the action of $\hat{U}(1,0,0)$ since $\hat{U}(j,0,0) = \hat{U}(1,0,0)^j$. For this purpose, we utilize the multiplication rule: $P(0,m',n')P(1,0,0) = P(1,0,0)P(0,m,n)$ [41], or equivalently,

$$\hat{U}(0,m',n')\hat{U}(1,0,0) = \hat{U}(1,0,0)\hat{U}(0,m,n), \tag{3}$$

where $(m',n')^T = A\,(m,n)^T$. Acting both sides of Eq. (3) on $|k,\alpha\rangle$, we find that $\hat{U}(1,0,0)|k,\alpha\rangle$ is also an eigenstate of translation operators, denoted by $|k',\alpha'\rangle = \hat{U}(1,0,0)|k,\alpha\rangle$ without loss of generality. And Eq. (3) determines a relation between k and k' [41], which reads

$$\begin{pmatrix} k' \\ E_{\alpha'}(k') \end{pmatrix} = \bar{A}\begin{pmatrix} k \\ E_\alpha(k) \end{pmatrix} \pmod{2\pi}, \tag{4}$$

where $\bar{A} = \det(A)\,A$. Especially, we find $\bar{A} = -A$ and $\bar{A} = A$ for the symmetry classes $\mathcal{P}_2$ and $\mathcal{P}_4$, respectively. The modulo operation in Eq. (4) ensures that $(k',E_{\alpha'}(k'))$ falls within the FBBZ. According to definition, $\bar{A}$ is invertible, and then it is a one-to-one continuous map between FBBZ and itself. In other words, $\bar{A}$ acts as a homeomorphism on the FBBZ.

Equation (4) reveals that each point $(k,E_\alpha(k))$ within the DRs is mapped by $\bar{A}$ to another point within the DRs. $\bar{A}$ establishes a one-to-one correspondence between the set of points within the DRs and itself. In a spacetime crystal with N continuous bands, each with its corresponding DR as a loop on the FBBZ torus, $\bar{A}$ acts as a homeomorphism. Consequently, the image of a loop (DR) under $\bar{A}$ is guaranteed to be another loop (DR). Thus, $\bar{A}$ maps each DR loop to another DR loop, effectively acting as a permutation of the N bands.

Topology of dispersion relation.— Equation (4) is the sufficient and necessary condition for a unitary representation of $\mathcal{P}_M$. Constructing a representation involves in finding the $\bar{A}$-invariant DRs (solution of Eq. (4)). For general $\bar{A}$, these DRs can be highly nontrivial. For instance, if A is the exchange A_e, then $\bar{A}_e$ exchanges the quasi-momentum and quasi-energy. Our familiar DRs, such as quadratic or trigonometric functions, are not $\bar{A}$-invariant. The nontriviality of $\bar{A}$-invariant DRs arises from the fact that their loops exhibit nontrivial topology. The topology of a loop on a torus is characterized by a pair of integers, which corresponds to the fundamental group of the torus. As the DR is a continuous function of k within the range of $[-\pi,\pi)$, a DR loop must wind around the torus exactly once in the k-direction. The topology of a DR loop is denoted as $(1,w)$, where w represents the number of times the DR winds around the torus in the positive E-direction while completing one revolution in the positive k-direction. It is important to highlight that w has long been recognized as the average particle displacement over one period. In each cycle, w units of charge are pumped through the system [2].

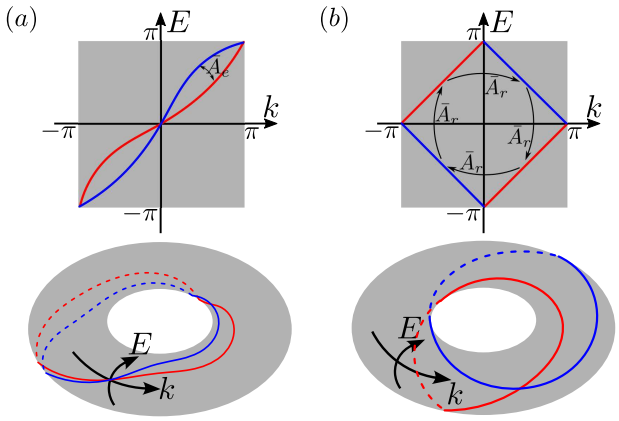


FIG. 2. The blue and red lines represent a doublet, consisting of a pair of DRs that are mutually mapped by (a) $\bar{A}_e$ (exchange transformation) and (b) $\bar{A}_r$ (rotation transformation). The bottom panels schematically depict the topological equivalence of these doublets on the FBBZ torus.

If $\bar{A}$ maps band α to α', their DRs' winding numbers (w_α and $w_{\alpha'}$) are connected to each other according to [41]

$$\pm\begin{pmatrix} 1 \\ w_{\alpha'} \end{pmatrix} = \bar{A}\begin{pmatrix} 1 \\ w_\alpha \end{pmatrix}. \tag{5}$$

Equation (5) is our key result, which constrains the topology of an $\bar{A}$-invariant DR. It has no solution for $\bar{A}$ in $\mathcal{P}_3$ or $\mathcal{P}_6$ [41], indicating that these symmetry classes have no representation with continuous bands. By substituting the expression of A into Eq. (5), we obtain the band classification for $\mathcal{P}_2$ and $\mathcal{P}_4$. In $\mathcal{P}_2$, bands are classified as singlets or doublets. A singlet remains invariant under $\bar{A}$, while a doublet consists of two bands mapped by $\bar{A}$ into each other, sharing the same winding number. For $\mathcal{P}_4$, bands are classified as doublets with odd-function DRs of k and quadruplets (quartets of four bands). There are no singlet bands since $w_{\alpha'} = w_\alpha$ constradicts Eq. (5). Additionally, the two bands in a doublet have different winding numbers. Table I summarizes the classification of Floquet-Bloch bands with mixing symmetry.

Except for A with $a = \pm 1$ (unconventional space inversion or time reversal), the DR's winding number must be nonzero [41]. Figure 2 presents examples of DRs that satisfy Eq. (5). Figure 2(a) shows a doublet pair of bands, mapped

into each other by $\bar{A}_e$ in $\mathcal{P}_2$. Both bands have a winding number of +1. Figure 2(b) shows a doublet pair of bands, mapped into each other by $\bar{A}_r$ in $\mathcal{P}_4$. The two bands have winding numbers of +1 and −1, respectively.

The simplest DRs with mixing symmetries (solution of Eq. (4)) are linear ones: $E(k) = wk$, where $w = \pm 1, \pm 2, \cdots$ represents the winding number. From Eqs. (4) and (5), we can fully determine the mixing symmetries of any linear Floquet-Bloch band [41]. In the $\mathcal{P}_2$ symmetry class, a linear band is a singlet, which keeps invariant under the map $\bar{A}$ with elements satisfying $a = -bw \pm 1$ and $c = -bw^2 \pm 2w$. On the other hand, in the $\mathcal{P}_4$ symmetry class, two bands $E(k) = wk$ and $E'(k) = w'k$ can form a doublet, where $w' = w \pm 1$ or $w' = w \pm 2$ [41].

By utilizing the $\bar{A}$-invariant $E_\alpha(k)$, we can readily establish the many-body quantum theory by introducing the creation operator $\hat{c}^\dagger_{k,\alpha}$ and the annihilation operator $\hat{c}_{k,\alpha}$ and expressing the symmetry operators in terms of them [37]. Specifically, the time translation operator is $\hat{U}(0,1,0) = e^{i\hat{H}_F}$, where $\hat{H}_F$ is the effective Floquet Hamiltonian:

$$\hat{H}_F = \sum_{k,\alpha} E_\alpha(k)\, \hat{c}^\dagger_{k,\alpha} \hat{c}_{k,\alpha}. \tag{6}$$

Note that the symmetry condition of DRs is independent of whether the particles are bosons or fermions. The operators $\hat{c}_{k,\alpha}, \hat{c}^\dagger_{k,\alpha}$ are either commutative or anti-commutative, depending on the species of particles.

A few comments are necessary. First, we ignore the interaction between particles in the model (6). Constructing an interacting theory is significantly more challenging and falls beyond the scope of the current paper, as the mixing symmetry imposes constraints not only on the DR but also on the particle interactions. Second, for an exhaustive enumeration of quantum theories, we should also consider the possibility of $\hat{U}(1,0,0)$ being an anti-unitary operator, which is discussed in the supplementary materials.

Realization with local $\hat{H}(t)$.— We aim at realize a given Floquet Hamiltonian $\hat{H}_F$, or equivalently the energy band $E(k)$, in a cold atom system on an optical lattice. To achieve experimental feasibility, it is crucial that the time-periodic Hamiltonian $\hat{H}(t)$ possesses locality in real spacetime. However, this poses a challenge due to the nonzero winding numbers of the DRs, which is a characteristic feature of mixing symmetry.

Let us consider a specific example: the linear DRs $E(k) = wk$. Upon Fourier transformation, the Floquet Hamiltonian $\hat{H}_F$ contains infinitely-long-range hopping terms in real space, making them currently inaccessible using existing technology. In fact, if $\hat{H}(t)$ exhibits locality (i.e., short-range hopping) and simultaneously maintains space translational symmetry at each time t, then the DRs of $\hat{H}_F$ must possess zero winding [41]. Therefore, in order to have an $\bar{A}$-invariant DR, $\hat{H}(t)$ must break instantaneous translational symmetry.

To design $\hat{H}(t)$ for a given DR, we employ the recently developed QQFT protocol [38], which gives rise to highly flexible Hamiltonian engineering so that the DRs become completely programmable and the long-range tunnelings in $\hat{H}_F$ become accessible to optical lattice experiments. In one period, denoted as $[0, 1)$, the time-dependent Hamiltonian is expressed as

$$\hat{H}(t) = \sum_{p=1}^{D} I_p(t)\, \hat{H}_p. \tag{7}$$

Here, $I_p(t)$ is the indicator function, which is defined as 1 for $t \in [(p-1)/D, p/D)$ and zero elsewhere. The parameter D represents the depth of the Hamiltonian sequence. Each $\hat{H}_p$ contains only onsite potentials and nearest-neighbor hoppings. It can generally be written as $\hat{H}_p = \sum_x \left(g^{(p)}_x \hat{\psi}^\dagger_x \hat{\psi}_{x+1} + u^{(p)}_x \hat{\psi}^\dagger_x \hat{\psi}_x + h.c. \right)$, where $\hat{\psi}^\dagger_x$ and $\hat{\psi}_x$ are the creation and annihilation operators at site x, respectively, and g and u denote the hopping strength and onsite potentials, respectively. The unitary evolution over one period is given by $e^{-i\hat{H}_F} = e^{-i\hat{H}_D/D} \cdots e^{-i\hat{H}_2/D} e^{-i\hat{H}_1/D}$. For a lattice model with L sites, the depth D scales as $L \log L$ for large L [38], in the QQFT protocol. As the system size increases, the effort required for simulation grows super-linearly. In recent developments in cold atom technology, spatially resolved control of the atom-confining potential has been achieved, enabling the realization of a sequence of local Hamiltonians like Eq. (7). It has been shown that systems with sizes up to several tens of sites are accessible in present experiments [38, 43].

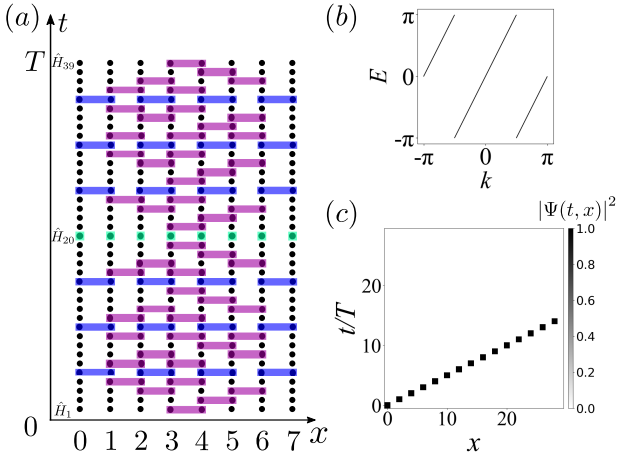


FIG. 3. (a) The sequence of $\hat{H}_p$ operations with $p = 1, \cdots, 39$ in one period ($t \in [0, T]$) for a lattice of size $L = 8$. The lattice sites, labeled as $0 \sim 7$, are represented by black dots. The purple and blue rectangles depict the swap and local Fourier operations between neighboring sites, respectively. The green squares represent the onsite-potential operation. (b) The linear dispersion relation $E = 2k$. (c) The probability density $|\Psi(t,x)|^2$ as a particle propagates.

Figure 3(a) illustrates the sequence of $\hat{H}_p$ operations that generate $E(k) = wk$ on a chain of length $L = 8$. Within each period, a total of 39 operations are performed, including 32 swaps between neighboring sites, 6 local Fourier transformations, and one evolution of the onsite potential. For more detailed information, please refer to the supplemental material.

Mixing symmetry in the wave function.— To observe the mixing symmetry, one can utilize the fact that the mixing symmetry manifests itself in the particle propagator in real spacetime. For a particle initially located at position $x = 0$ and time $t = 0$, its wave function at a later time (multiples of the period) satisfies:

$$\Psi_\alpha(t, x) = \Psi_{\alpha'}(t', x'), \tag{8}$$

where $(t', x')^T = A\,(t, x)^T$ and t, x are arbitrary integers. α' is the map of band-α under $\bar{A}$. For $\alpha' = \alpha$ (a singlet band in the $\mathcal{P}_2$ class), Eq. (8) imposes a strong constraint on the wave function. For $\alpha' \neq \alpha$, Eq. (8) provides a connection between the wave functions in different bands.

For a concrete example, let us see a linear band with $E(k) = wk$, in which the particle moves at a constant speed, just like a classical particle. The wave function is calculated to be $\Psi_\alpha(t, x) = \delta_{x,wt}$. In previous discussions, we already show that such a band exhibits the $\mathcal{P}_2$ symmetry when the elements of A are $a = -bw \pm 1$ and $c = -bw^2 \pm 2w$. It is easy to verify that $\delta_{x,wt}$ does remain invariant as $(t, x)^T$ transforms under A. Using the QQFT protocol, we perfectly repeat the evolution of wave function on a lattice of length $L = 2^l$. Figure 3(b) displays the DR as $w = 2$, and Fig. 3(c) displays the corresponding wave function in the QQFT simulation.

The probability distribution of particles, i.e. $|\Psi(t, x)|^2$, obviously meets the same symmetry as shown in Eq. (8). In experiments, instead of a single particle, one can use the Bose-Einstein condensate (BEC) for observation, and then, $|\Psi(t, x)|^2$ represents the density of atoms. The density distribution forms a symmetric pattern which remains invariant under A, which will be a smoking gun signal of mixing symmetry.

Discussion.— This paper presents an innovative discovery of Floquet-Bloch band theories that exhibit a unique mixing symmetry, which intertwines the space and time coordinates. We provide a comprehensive classification of Floquet-Bloch bands based on the cyclic mixing transformations of finite order. Notably, only the groups $\mathcal{P}_2$ and $\mathcal{P}_4$ possess continuous representations, where the mixing symmetry imposes constraints on the dispersion relation of each band. Furthermore, we reveal that the winding number of the dispersion relation on the Floquet-Bloch-Brillouin torus must adhere to a symmetry condition. To achieve a non-zero winding number, it is essential for the time-dependent Hamiltonian of the theory to break the instantaneous translation symmetry, a feat attainable through the implementation of QQFT on an optical lattice. Remarkably, the mixing symmetry manifests in the atom density, which becomes experimentally measurable, demonstrating its impact on the spacetime distribution. This discovery unveils a broader symmetry family that has been previously ignored, as the mixing symmetry transcends pure spatial or temporal characteristics and instead establishes correlations between space and time. Its exploration enhances our comprehension of symmetry in crystals. Looking ahead, intriguing open questions include the investigation of noncyclic mixing symmetry and the exploration of mixing-symmetry protected topological states of matter.

Acknowledgement.— The work is supported by National Natural Science Foundation of China (Grants Nos. 11835011, 11774315), and the Junior Associates program of the Abdus Salam International Center for Theoretical Physics. We thank X. Wang for useful discussions.

* wangpei@zjnu.cn

[1] T. Oka and H. Aoki, Phys. Rev. B **79**, 081406(R) (2009).
[2] T. Kitagawa, E. Berg, M. Rudner, and E. Demler, Phys. Rev. B **82**, 235114 (2010).
[3] N. H. Lindner, G. Refael, and V. Galitski, Nat. Phys. **7**, 490 (2011).
[4] N. R. Cooper, J. Dalibard, and I. B. Spielman, Rev. Mod. Phys. **91**, 015005 (2019).
[5] M. S. Rudner and N. H. Lindner, Nat. Rev. Phys. **2**, 229 (2020).
[6] M. C. Rechtsman, J. M. Zeuner, Y. Plotnik, Y. Lumer, S. Nolte, M. Segev, and A. Szameit, Nature **496**, 196 (2013).
[7] Y. H. Wang, H. Steinberg, P. Jarillo-Herrero, and N. Gedik, Science **342**, 453 (2013).
[8] G. Jotzu, M. Messer, R. Desbuquois, M. Lebrat, T. Uehlinger, D. Greif, and T. Esslinger, Nature **515**, 237 (2014).
[9] A. S. Sørensen, E. Demler, and M. D. Lukin. Phys. Rev. Lett. **94**, 086803 (2005).
[10] A. Eckardt, C. Weiss, and M. Holthaus, Phys. Rev. Lett. **95**, 260404 (2005).
[11] N. Goldman and J. Dalibard, Phys. Rev. X **4**, 031027 (2014).
[12] T. Oka and S. Kitamura, Annu. Rev. Condens. Matter Phys. **10**, 387 (2019).
[13] D. V. Else, B. Bauer, and C. Nayak, Phys. Rev. Lett. **117**, 090402 (2016).
[14] V. Khemani, A. Lazarides, R. Moessner, and S. L. Sondhi, Phys. Rev. Lett. **116**, 250401 (2016).
[15] N. Y. Yao, A. C. Potter, I.-D. Potirniche, and A. Vishwanath, Phys. Rev. Lett. **118**, 030401 (2017).
[16] P. Ponte, Z. Papić, F. Huveneers, and D. A. Abanin, Phys. Rev. Lett. **114**, 140401 (2015).
[17] A. Lazarides, A. Das, and R. Moessner, Phys. Rev. Lett. **115**, 030402 (2015).
[18] P. Bordia, H. Lüschen, U. Schneider, M. Knap, and I. Bloch, Nat. Phys. **13**, 460 (2017).
[19] M. S. Rudner, N. H. Lindner, E. Berg, and M. Levin, Phys. Rev. X **3**, 031005 (2013).
[20] N. W. Ashcroft and N. D. Mermin, *Solid state physics* (Tomson Learning Inc., London, UK, 1976).
[21] A. Altland and M. R. Zirnbauer, Phys. Rev. B **55**, 1142 (1997).
[22] A. P. Schnyder, S. Ryu, A. Furusaki, and A. W. W. Ludwig, Phys. Rev. B **78**, 195125 (2008).
[23] A. Kitaev, AIP Conf. Proc. **1134**, 22 (2009).
[24] F. Nathan and M. S Rudner, New J. Phys. **17**, 125014 (2015).
[25] A. C. Potter, T. Morimoto, and A. Vishwanath, Phys. Rev. X **6**, 041001 (2016).
[26] D. V. Else and C. Nayak, Phys. Rev. B **93**, 201103(R) (2016).
[27] R. Roy and F. Harper, Phys. Rev. B **96**, 155118 (2017).
[28] B. Bradlyn, L. Elcoro, J. Cano, M. G. Vergniory, Z. Wang, C. Felser, M. I. Aroyo, and B. A. Bernevig, Nature **547**, 298 (2017).
[29] H. C. Po, A. Vishwanath, and H. Watanabe, Nat. Commun. **8**, 50 (2017).
[30] J. Kruthoff, J. de Boer, J. van Wezel, C. L. Kane, and R.-J. Slager, Phys. Rev. X **7**, 041069 (2017).

[31] T. Morimoto, H. C. Po, and A. Vishwanath, Phys. Rev. B **95**, 195155 (2017).
[32] S. Xu and C. Wu, Phys. Rev. Lett. **120**, 096401 (2018).
[33] Y. Peng and G. Refael, Phys. Rev. Lett. **123**, 016806 (2019).
[34] K. Mochizuki, T. Bessho, M. Sato, and H. Obuse, Phys. Rev. B **102**, 035418 (2020).
[35] P. Wang, New J. Phys. **20**, 023042 (2018).
[36] X. Li, J. Chai, H. Zhu, and P. Wang, J. Phys.: Condens. Matter **32**, 145402 (2020).
[37] P. Wang, J. Phys. A: Math. Theor. **54**, 115003 (2021).
[38] P. Wang, Z. Huang, X. Qiu, and X. Li, Phys. Rev. B **106**, 134313 (2022).
[39] Y. Wang, A. Kumar, T.-Y. Wu, and D. S. Weiss, Science **352**, 1562 (2016).
[40] A. Browaeys and T. Lahaye, Nat. Phys. **16**, 132 (2020).
[41] See Supplementary Materials.
[42] S. Weinberg, *The Quantum Theory of Fields* (Cambridge University Press, Cambridge, England, 1995).
[43] X. Qiu, J. Zou, X. Qi, and X. Li, npj Quantum Inf. **6**, 87 (2020).

Supplementary Materials

S-1. MIXING GROUPS

According to definition, the mixing symmetry group has two important subgroups. One is the cyclic group that contains the mixing transformations, i.e., $\mathcal{A} = \left\{1, A, A^2, \cdots, A^{M-1}\right\}$ with M being the order. The other consists of the translations, reading $\mathcal{T} = \{(m,n)\,|m,n \in \mathbb{Z}\}$. Usually, the group that has $\mathcal{A}$ and $\mathcal{T}$ as subgroups is not unique. In this paper, we only consider the symmorphic group, which is the direct product of $\mathcal{A}$ and $\mathcal{T}$. The group element is written as $P(j,m,n)$, which represents the mixing transformation A^j followed by the translation of vector (m,n). It is easy to see that, $\mathcal{P} = \{P(j,m,n)\}$ is a group if and only if the spacetime lattice $\mathcal{T}$ keeps invariant under A. Because A is invertible ($A^{-1} = A^{M-1}$), $\mathcal{T}$ keeps invariant under A if and only if m' and n', defined by $(m',n')^T = A\,(m,n)^T$, are integers for arbitrary $m,n \in \mathbb{Z}$. Furthermore, this condition can be simplified into $A\,(1,0)^T$ and $A\,(0,1)^T$ being integer pairs.

We generally express the matrix A and its inverse as

$$A = \begin{pmatrix} a_{11} & a_{12} \\ a_{21} & a_{22} \end{pmatrix} \quad \text{and} \quad A^{-1} = \frac{1}{\det(A)} \begin{pmatrix} a_{22} & -a_{12} \\ -a_{21} & a_{11} \end{pmatrix}, \tag{S1}$$

respectively. Then, the condition that $A\,(1,0)^T$ and $A\,(0,1)^T$ are integer pairs translates into $a_{11}, a_{12}, a_{21}, a_{22}$ being all integers. But $A^j\,(1,0)^T$ and $A^j\,(1,0)^T$ must be also integer pairs for $j = 2,3,\cdots,M-1$. The case of $j = M-1$, or equivalently $j = -1$, is especially important, from which we derive that $a_{11}/\det(A), a_{12}/\det(A), a_{21}/\det(A), a_{22}/\det(A)$ are integers. For a_{ij} and $a_{ij}/\det(A)$ to be both integers, we require $\det(A) = \pm 1$. To see it, one can use proof by contradiction (the assumption $\det(A) = \pm 2, \pm 3, \cdots$ leads to contradiction).

To find all the cyclic As, we study the eigenvalues of A, i.e. a pair of complex numbers expressed as $\lambda_\pm = \frac{a_{11}+a_{22}}{2} \pm \sqrt{\left(\frac{a_{11}+a_{22}}{2}\right)^2 - \det(A)}$. The cyclic condition ($A^M = 1$) indicates $|\lambda_\pm| \equiv 1$, which is possible only if $a_{11} + a_{22} = 0, \pm 1, \pm 2$. As $a_{11} + a_{22} = 0$ and $\det(A) = -1$, a straightforward calculation shows $A^2 = 1$. Such As can be written in a more compact form as

$$A = \begin{pmatrix} a & b \\ c & -a \end{pmatrix}, \tag{S2}$$

where a, b, c are arbitrary integers satisfying $bc = -a^2 + 1$. As $a_{11} + a_{22} = 0$ and $\det(A) = +1$, we find $A^4 = 1$, and A has the same expression as Eq. (S2) but with $bc = -a^2 - 1$. As $a_{11} + a_{22} = \pm 1$, only $\det(A) = 1$ is consistent with $|\lambda_\pm| \equiv 1$ but $\det(A) = -1$ is not, and we find $A^6 = 1$ or $A^3 = 1$, respectively. As $a_{11} + a_{22} = \pm 2$, the calculation shows that there does not exist a finite M so that $A^M = 1$, except for $A = \pm 1$, which is trivial and then ignored.

To summarize, the values of M are $2, 3, 4$ or 6, and the corresponding symmetry groups are denoted by $\mathcal{P}_2, \mathcal{P}_3, \mathcal{P}_4$ or $\mathcal{P}_6$, respectively. For a given M, $\mathcal{P}_M$ is a class of groups, with different groups having different A. In $\mathcal{P}_2$, A is the matrix (S2) with $bc = -a^2 + 1$. In $\mathcal{P}_4$, A is the matrix (S2) with $bc = -a^2 - 1$. In $\mathcal{P}_3$, A is the matrix (S1) with the components being arbitrary integers that satisfy $a_{11} + a_{22} = -1$ and $a_{11}a_{22} - a_{12}a_{21} = 1$. In $\mathcal{P}_6$, A is the matrix (S1) with the components being arbitrary integers that satisfy $a_{11} + a_{22} = +1$ and $a_{11}a_{22} - a_{12}a_{21} = 1$.

S-2. UNITARY AND ANTI-UNITARY REPRESENTATIONS

We use $|k,\alpha\rangle$ to denote the single-particle eigenstate of the translation operators $\hat{U}(0,m,n)$ with $m,n \in \mathbb{Z}$. According to the Floquet-Bloch band theory, without loss of generality, the corresponding eigenvalue can be expressed as $e^{imE_\alpha(k)-ikn}$, where k and $E_\alpha(k)$ are the quasi-momentum and quasi-energy, respectively, and α is the band index. Let us calculate $\hat{U}(1,0,0)\,|k,\alpha\rangle$. From the definition of $P(j,m,n)$, it is easy see $P(0,m',n')P(1,0,0) = P(1,0,0)P(0,m,n)$ with $(m',n')^T = A\,(m,n)^T$. $\hat{U}(j,m,n)$ is the representation of $P(j,m,n)$, then they satisfy the same multiplication rule. We obtain

$$\hat{U}(0,m',n')\hat{U}(1,0,0)\,|k,\alpha\rangle = \hat{U}(1,0,0)\hat{U}(0,m,n)\,|k,\alpha\rangle = e^{imE_\alpha(k)-ikn}\hat{U}(1,0,0)\,|k,\alpha\rangle\,. \tag{S3}$$

Equation (S3) tells us that $\hat{U}(1,0,0)\,|k,\alpha\rangle$ is the eigenstate of $\hat{U}(0,m',n')$ with the eigenvalue being $e^{imE_\alpha(k)-ikn}$. But m' and n' can be arbitrary integers, because $(m',n')^T = A\,(m,n)^T$ and A is invertible. $\hat{U}(1,0,0)\,|k,\alpha\rangle$ is then the common eigenstate of the translation operators, denoted by $|k',\alpha'\rangle$ without loss of generality. Using the notations k' and α', we calculate the left-hand side of Eq. (S3) and then obtain

$$e^{im'E_{\alpha'}(k')-ik'n'} = e^{imE_\alpha(k)-ikn}. \tag{S4}$$

Using the fact that $\det(A) = \pm 1$ and the expression of A^{-1} in Eq. (S1), we quickly find

$$\begin{pmatrix} k' \\ E_{\alpha'}(k') \end{pmatrix} = \bar{A} \begin{pmatrix} k \\ E_{\alpha}(k) \end{pmatrix} \pmod{2\pi} \tag{S5}$$

with $\bar{A} = \det(A) \cdot A = \pm A$.

In the above derivation, we assume that $\hat{U}(1,0,0)$, i.e. the representation of A, is a unitary operator. To make our discussion complete, we also need to consider the possibility of $\hat{U}(1,0,0)$ being an anti-unitary operator. In this case, the multiplication rule keeps the same, but Eq. (S3) changes into $\hat{U}(0,m',n')\hat{U}(1,0,0)\,|k,\alpha\rangle = e^{-imE_\alpha(k)+ikn}\hat{U}(1,0,0)\,|k,\alpha\rangle$. Due to the reason mentioned above, we still assume $\hat{U}(1,0,0)\,|k,\alpha\rangle = |k',\alpha'\rangle$. Then Eq. (S4) becomes $e^{im'E_{\alpha'}(k')-ik'n'} = e^{-imE_\alpha(k)+ikn}$. Equation (S5) keeps the same but with $\bar{A} = -\det(A) \cdot A$. Comparing the anti-unitary representation with the unitary representation, we find that the dispersion relation satisfies the same equation with only the sign of $\bar{A}$ changing. On the other hand, if we do the change $A \to -A$ in the unitary representation, the sign of $\bar{A}$ also changes, since $\det(A) = \det(-A)$. Moreover, if A is a cyclic matrix, so is $-A$. Therefore, for each anti-unitary representation, there exists a unitary representation that has exactly the same $\bar{A}$, and then the dispersion relation, i.e. the solution of Eq. (S5), is also the same. The consideration of anti-unitary representation leads to nothing new in the dispersion relation.

S-3. TOPOLOGY OF DISPERSION RELATION

We assume that the Floquet-Bloch band is continuous, or in other words, $E_\alpha(k)$ is a continuous function of k everywhere in the Floquet-Bloch-Brillouin zone (FBBZ). The dispersion relation (DR) of each band is then a loop on the FBBZ torus. The transformation $\bar{A} \pmod{2\pi}$ defined by Eq. (S5) maps a point in the FBBZ to another point in the FBBZ. Furthermore, it is a one-to-one map. Otherwise, suppose $(k_1, E_1) \neq (k_2, E_2)$ are mapped into the same (k', E'), then we have $\bar{A}\,(k_1 - k_2, E_1 - E_2)^T = 2\pi\,(m,n)^T$ with m, n being some integers. But the matrix $\bar{A} = \pm A$ or its inverse always map an integer pair into another integer pair, and then $(k_1 - k_2, E_1 - E_2) = 2\pi\,(m', n')$ with m', n' being integers. This is impossible except for $k_1 = k_2$ and $E_1 = E_2$, because (k_1, E_1) and (k_2, E_2) are both in the FBBZ.

The one-to-one map $\bar{A}$ is by definition continuous, so is its inverse. $\bar{A}$ is then a homeomorphism. As a consequence, an arbitrary loop on the FBBZ torus must be mapped by $\bar{A}$ into another loop. In the main text, we show that the spacetime crystal has the mixing symmetry if and only if the single-particle DRs are $\bar{A}$-invariant. And if the DRs are $\bar{A}$-invariant, then the DR of a band α, i.e. a loop, must be mapped into the DR of another band α' (it is possible that $\alpha = \alpha'$). Note that, from the pure mathematical point of view, it is also possible that the image of a DR loop is a non-DR loop (e.g., a loop on which k keeps a constant but E travels around the torus once). But in that case, the DRs are not $\bar{A}$-invariant, and then the corresponding spacetime crystal has no mixing symmetry, which is uninteresting to us.

Next, we study the topologies of the DR loops of α and α'. Using the knowledge of the fundamental group of torus, we describe the topology of a loop by two integers, which are the numbers of times the loop winds around the torus in the positive k- and E-directions, respectively. A DR loop winds around the torus once and only once in the k-direction, otherwise, there would exist some $k \in [-\pi, \pi)$ at which $E(k)$ has no definition or has multiple values, which contradicts with the fact that $E(k)$ is a function of k defined in the domain $[-\pi, \pi)$. Therefore, the topology of the α-band DR is given by the pair $(1, w_\alpha)$, in which w_α is the number of times the loop winds in the positive-E direction as it winds once in the positive-k direction.

An easy way of calculating w_α is by depicting $E_\alpha(k)$ in the extended quasi-energy zone, in which the range of E is extended to $(-\infty, \infty)$ instead of being limited in $[-\pi, \pi)$. In the extended-zone scheme, we can force $E_\alpha(k)$ to be continuous in the absence of the modulo operation, $E_\alpha(k)$ then becomes a curve in the k-E plane with $k \in [-\pi, \pi)$ and $E \in (-\infty, \infty)$. The continuity of $E_\alpha(k) \pmod{2\pi}$ requires $(E_\alpha(\pi) - E_\alpha(-\pi))$ being an integer times of 2π, and this integer is exactly w_α:

$$E_\alpha(\pi) - E_\alpha(-\pi) = 2\pi w_\alpha. \tag{S6}$$

Now, we study the image of $\{(k, E_\alpha(k))\}$ under the matrix $\bar{A}$, in the extended-zone scheme. Without the modulo operation, $\bar{A}$ is an invertible one-to-one map in the k-E plane, moreover, it is a linear map. Therefore, when $(k, E_\alpha(k))$ starts from the left end $(-\pi, E_\alpha(-\pi))$, and goes towards the right end $(\pi, E_\alpha(\pi))$, its image $(k', E_{\alpha'}(k'))$ draws a curve in the plane. The end points of the image curve are $\left(k'_0, E_{\alpha'}(k'_0)\right)^T = \bar{A}\,(-\pi, E_\alpha(-\pi))^T$ and $\left(k'_1, E_{\alpha'}(k'_1)\right)^T = \bar{A}\,(\pi, E_\alpha(\pi))^T$, respectively. Then, the winding number of α' evaluates $w_{\alpha'} = \left(E_{\alpha'}(k'_1) - E_{\alpha'}(k'_0)\right) / \left(k'_1 - k'_0\right)$. An important property of the image curve is that $\left|k'_1 - k'_0\right|$ must be 2π. The proof is as follows. First, the range of k' must be integer times of 2π, because the image is a complete DR loop (of band α') after the modulo operation. Second, the range of k' cannot be $2\pi n$ with $n > 1$. Otherwise, as $(k, E_\alpha(k))$ travels around the α-DR loop once, $(k', E_{\alpha'}(k'))$ already travels around the α'-DR loop n times, which contradicts with the fact that $\bar{A} \pmod{2\pi}$ is a one-to-one

map on the torus. Based on the above arguments, we derive

$$\pm\begin{pmatrix} 1 \\ w_{\alpha'} \end{pmatrix} = \bar{A}\begin{pmatrix} 1 \\ w_{\alpha} \end{pmatrix}, \tag{S7}$$

where "±" corresponds to $k'_1 - k'_0 = \pm 2\pi$, respectively.

S-4. MIXING SYMMETRIES OF LINEAR $E(k)$

We determine the mixing symmetries of a linear DR, given by $E(k) = wk$ with $w = \pm 1, \pm 2, \cdots$, by making the following observation. If the topology condition $\pm (1, w')^T = \bar{A}\,(1, w)^T$ is satisfied, we can multiply both sides by k to obtain $(k', E')^T = \bar{A}\,(k, E)^T$, where $k' = \pm k$ and $E' = w'k'$. Therefore, the topology condition is sufficient for one linear band to be mapped by $\bar{A}$ into another linear band.

Let us first consider the $\mathcal{P}_2$ symmetry class. Since $w = w'$ under the map $\bar{A}$ (see Tab. I of the main text), a linear $E(k)$ is always mapped into itself and remains a singlet band in the $\mathcal{P}_2$ class. Using the equation $\pm (1, w)^T = \bar{A}\,(1, w)^T$ and the expression of $\bar{A}$, we immediately find $a = -bw \pm 1$ and $c = -bw^2 \pm 2w$. For a given w, there exist an infinite number of mixing matrices (with different b) in the $\mathcal{P}_2$ class:

$$A = \begin{pmatrix} -bw \pm 1 & b \\ -bw^2 \pm 2w & bw \mp 1 \end{pmatrix}. \tag{S8}$$

The linear band $E(k) = wk$ always exhibits $\mathcal{P}_2$ symmetries.

Next, we consider the $\mathcal{P}_4$ symmetry class. Since $E(k) = wk$ is an odd function of k, the linear band must be one branch of a doublet (Tab. I of the main text). Suppose the DR of its paired band is $E'(k') = w'k'$. Using $\pm (1, w')^T = \bar{A}\,(1, w)^T$ and the expression of $\bar{A}$, we find $a = -bw \pm 1$, $c = -bw^2 \pm 2w - 2/b$, and $w' = w \mp 2/b$. c and w' must be integers, therefore, b can only take the values $\pm 1, \pm 2$. For a given w, there exist 8 mixing matrices in the $\mathcal{P}_4$ symmetry class:

$$A = \begin{pmatrix} -w \pm 1 & 1 \\ -w^2 \pm 2w - 2 & w \mp 1 \end{pmatrix}, \begin{pmatrix} w \pm 1 & -1 \\ w^2 \pm 2w + 2 & -w \mp 1 \end{pmatrix}, \begin{pmatrix} -2w \pm 1 & 2 \\ -2w^2 \pm 2w - 1 & 2w \mp 1 \end{pmatrix}, \begin{pmatrix} 2w \pm 1 & -2 \\ 2w^2 \pm 2w + 1 & -2w \mp 1 \end{pmatrix}. \tag{S9}$$

The corresponding w' is given by $w' = w \mp 2, w \pm 2, w \mp 1, w \pm 1$, respectively.

The above analysis exhausts all the mixing symmetries of a linear band.

S-5. CONSTRUCTION OF $\hat{H}(t)$

Our target is to simulate $\hat{H}_F = \sum_k E(k)\,\hat{c}_k^\dagger \hat{c}_k$ that has mixing symmetry by a periodic Hamiltonian $\hat{H}(t)$ with locality. First, we will prove that, if $\hat{H}(t)$ has both locality and space translation symmetry at each t, then the winding number of $E(k)$ is zero. For simplicity, we consider a lattice model, in which a set of sites are spatially located at the coordinates $j = 0, \pm 1, \pm 2, \cdots$, respectively. In condensed matter community, the lattice models are widely employed in the study of particles moving in a periodic potential, because it is more difficult to directly deal with the differential operators in the continuous space. Without loss of generality, we define

$$\hat{H}(t) = \sum_j \sum_{\Delta j=-R}^{R} f(\Delta j, t)\hat{\psi}_j^\dagger \hat{\psi}_{j+\Delta j}, \tag{S10}$$

where $f(\Delta j, t) = f^*(-\Delta j, t)$ is the hopping strength, and $\hat{\psi}^\dagger$ and $\hat{\psi}$ are the onsite creation and annihilation operators, respectively. The assumption that $\hat{H}(t)$ has space translation symmetry at each moment, is hidden in the fact that $f(t)$ is independent of j. The locality of $\hat{H}(t)$ manifests itself as the existence of a distance cutoff for hopping. The largest distance over which there are nonzero hopping terms is set to be R. After a Fourier transform, Eq. (S10) changes into $\hat{H}(t) = \sum_k E(k, t)\hat{\psi}_k^\dagger \hat{\psi}_k$, where $E(k, t) = \sum_{\Delta j=-R}^{R} f(\Delta j, t)e^{ik\Delta j}$. $E(k, t)$ is a sum of finite number of terms, with each term being a trigonometric function of k. If we depict these trigonometric functions on the FBBZ torus, they all have zero winding number, and then their sum, i.e. $E(k, t)$, must also have zero winding number. The Floquet Hamiltonian $\hat{H}_F$ can be obtained by integrating $\hat{H}(t)$ over one period. Because $\hat{H}(t)$ at different t commutes with each other. Then we obtain $E(k) = \int_0^T dt\, E(k, t)/T$ where $T = 1$ is the period. Since $E(k, t)$ at each t has zero winding, $E(k)$ must also have zero winding.

The DRs of a spacetime crystal with mixing symmetry usually have nonzero winding. And due to the above arguments, if we ask $\hat{H}(t)$ to be local and we want to simulate a $\hat{H}_F$ with nonzero-winding DRs, we need to break the instantaneous translation symmetry in $\hat{H}(t)$. In previous theoretical or experimental studies, people often focus on the atom-confining potential that keeps the instantaneous translation symmetry. This explains why the mixing symmetry has not been observed accidentally. The recently developed digital-micromirror-device and sub-wavelength techniques have realized programmable instantaneous-translation-symmetry-breaking potentials in the cold atomic gases. This provides the foundation for experimentally realizing $\hat{H}(t)$.

Because we already know the DRs of $\hat{H}_F$, the quadratic quantum Fourier transform (QQFT) protocol is especially useful for designing $\hat{H}(t)$ [38]. Here we briefly review the idea of QQFT. The Floquet Hamiltonian is defined by the fact that $e^{-i\hat{H}_F}$ is the evolution operator of quantum state over one time period. The QQFT protocol gives a sequence of local Hamiltonians, denoted by $\hat{H}_1, \hat{H}_2, \cdots \hat{H}_D$, which are consecutively engineered so that the evolution operator can be factorized as $e^{-i\hat{H}_F} = e^{-i\hat{H}_D/D} \cdots e^{-i\hat{H}_2/D} e^{-i\hat{H}_1/D}$, where D is the depth of the Hamiltonian sequence and $1/D$ is the lifetime of each Hamiltonian. To obtain the $\hat{H}_p$s, we utilize the fact that $\hat{H}_F = \sum_k E(k)\hat{c}_k^\dagger \hat{c}_k$ is quadratic. On a lattice of size L, we perform the Fourier transform $\hat{c}_k^\dagger = \sum_j \frac{e^{ikj}}{\sqrt{L}} \hat{\psi}_j^\dagger$ with $\hat{\psi}_j^\dagger$ being the onsite creation operator, and then reexpress the Floquet Hamiltonian as $\hat{H}_F = \hat{\Psi}^\dagger \mathcal{H} \hat{\Psi}$, where $\hat{\Psi}$ is the array of $\hat{\psi}_j$s and $\mathcal{H}$ is a Hermitian matrix with the elements being

$$\mathcal{H}_{j,j'} = \sum_k E(k) \frac{e^{ik(j-j')}}{L}. \tag{S11}$$

To proceed, we exploit a formula of quadratic-exponent operators, which can be easily derived from the Baker-Campbell-Hausdorff formula. For arbitrary Hermitian matrices $\mathcal{H}_1, \mathcal{H}_1, \cdots \mathcal{H}_d$ and a single Hermitian matrix $\mathcal{H}$ that satisfy

$$e^{-i\mathcal{H}_d} \cdots e^{-i\mathcal{H}_2} e^{-i\mathcal{H}_1} = e^{-i\mathcal{H}}, \tag{S12}$$

we always have

$$e^{-i\hat{\Psi}^\dagger \mathcal{H}_d \hat{\Psi}} \cdots e^{-i\hat{\Psi}^\dagger \mathcal{H}_2 \hat{\Psi}} e^{-i\hat{\Psi}^\dagger \mathcal{H}_1 \hat{\Psi}} = e^{-i\hat{\Psi}^\dagger \mathcal{H} \hat{\Psi}}. \tag{S13}$$

Equation (S13) simply says that the factorization of an evolution operator with quadratic Hamiltonian (such as $e^{-i\hat{H}_F}$) is equivalent to the factorization of the corresponding unitary matrix $e^{-i\mathcal{H}}$. To make $\hat{H}_p = \hat{\Psi}^\dagger \mathcal{H}_p \hat{\Psi}$ a local Hamiltonian, we need to ask the L-by-L matrix $\mathcal{H}_p$ to be local. In the QQFT protocol, each $\mathcal{H}_p$ contains only the diagonal elements (onsite potentials) and the off-diagonal elements $\mathcal{H}_{j,j+1}$ (hopping between nearest-neighbor sites). Observing Eq. (S11), we immediately find the next factorization:

$$e^{-i\mathcal{H}} = e^{-ie^{i\mathcal{F}} \mathcal{E} e^{-i\mathcal{F}}} = e^{i\mathcal{F}} e^{-i\mathcal{E}} e^{-i\mathcal{F}}, \tag{S14}$$

where $\mathcal{E}$ is a diagonal matrix with the diagonal elements being $E(k)$, and $\mathcal{F}$ is defined by $\left(e^{i\mathcal{F}}\right)_{j,j'} = \frac{1}{\sqrt{L}} e^{i2\pi jj'/L}$. In Eq. (S14), $\mathcal{E}$ is already diagonal and then satisfies the locality condition. Furthermore, $e^{i\mathcal{F}}$ is recognized to be the Fourier transformation, which can then be factorized into a sequence of local unitary matrices by using the algorithm of quantum Fourier transform (see Ref. [38] for the detail). The factorization of $e^{i\mathcal{F}}$ depends only upon the value of L. The analytical expressions of $\mathcal{H}_p$s have been obtained, as L is an integer power of 2, i.e. $L = 2^l$. The sequence depth of $e^{i\mathcal{F}}$ scales as $L \ln L$.

As an example, we give the sequence of Hamiltonians that generate the required dispersion relation on a one-dimensional lattice of length $L = 2^3 = 8$. For simplicity, we label the lattice sites as $j = 0, 1, \cdots, 7$. In this case, the unitary evolution over a single period can be factorized into

$$e^{-i\mathcal{H}} = R^{(2)} A^{(2)} R^{(2)\dagger} R^{(1)} A^{(1)} R^{(2)\dagger} A^{(0)} R^{(2)\dagger} e^{-i\mathcal{E}} R^{(2)} A^{(0)\dagger} R^{(2)} A^{(1)\dagger} R^{(1)\dagger} R^{(2)} A^{(2)\dagger} R^{(2)\dagger}. \tag{S15}$$

Here, $R^{(1)}$ and $R^{(2)}$ are the permutation matrices, which are realized by using a sequence of swaps, say $R^{(1)} = S^{(1,2)} S^{(5,6)}$ and $R^{(2)} = S^{(3,4)} S^{(4,5)} S^{(5,6)} S^{(2,3)} S^{(3,4)} S^{(1,2)}$, respectively. $S^{(j,j+1)}$ is the swap (the Pauli matrix σ_x) between two neighbor sites j and $j+1$. For the realization of $S^{(j,j+1)}$, the corresponding Hamiltonian is $h_{j,j+1} = h_{j+1,j} = -h_{j,j} = -h_{j+1,j+1} = \pi/2$ and $h_{i,i'} = 0$ for $i, i' \neq j, j+1$ (it is easy to verify $S^{(j,j+1)} = e^{-ih}$). The Hamiltonian h is definitely a local one, involving only an operation on two neighbor sites. $A^{(q)}$ with $q = 0, 1, 2$ is the local Fourier matrix, which couples $2j$ with $2j+1$ sites for $j = 0, 1, 2, 3$. Its nonzero matrix elements are

$$\begin{pmatrix} A^{(q)}_{2j,2j} = \frac{1}{\sqrt{2}} & A^{(q)}_{2j,2j+1} = \frac{1}{\sqrt{2}} e^{i2\pi(j\%2^q)/2^{q+1}} \\ A^{(q)}_{2j+1,2j} = \frac{1}{\sqrt{2}} & A^{(q)}_{2j+1,2j+1} = -\frac{1}{\sqrt{2}} e^{i2\pi(j\%2^q)/2^{q+1}} \end{pmatrix}, \tag{S16}$$

where % denotes the remainder. The corresponding Hamiltonian, i.e. $i\ln[A^{(q)}]$, has only the couplings between two nearest-neighbor sites. Finally, the Hamiltonian $\mathcal{E}$ in Eq. (S15) is made of the on-site potentials. For a linear dispersion $E(k) = wk$, the elements of $\mathcal{E}$ can be written as $\mathcal{E}_{i,j} = \delta_{i,j}\frac{2\pi}{L}jw$. One can also use the modulo 2π operation to force $\mathcal{E}_{i,j}$ to be in the interval $[-\pi, \pi)$. In the construction of the Hamiltonian sequence, we notice that multiple swaps that are commutative with each other can be combined into one without breaking the locality of Hamiltonian. For example, $S^{(1,2)}$ and $S^{(5,6)}$ in $R^{(1)}$ can be realized by using a single Hamiltonian that has the coupling between site-1 and site-2 and at the same time, also the coupling between site-5 and site-6. Such a consideration reduces the depth of the Hamiltonian sequence. In the case of $L = 8$, we find the depth to be $D = 39$. The sequence consists of 32 swaps, six $A^{(q)}$ and one $e^{-i\mathcal{E}}$.

S-6. MIXING SYMMETRY OF THE SINGLE-PARTICLE PROPAGATOR

In the main text, we derived from the multiplication rule that $|k', \alpha'\rangle = \hat{U}(1,0,0)\,|k, \alpha\rangle$, which illustrates the transformation of a single-particle state under $\hat{U}(1,0,0)$. In the language of many-body physics, it is more convenient to define $\hat{U}(1,0,0)$ based on its action on the creation or annihilation operators. This can be expressed as $\hat{c}^\dagger_{k'\alpha'} = \hat{U}(1,0,0)\hat{c}^\dagger_{k\alpha}\hat{U}^\dagger(1,0,0)$. The field operators in real space are obtained through Fourier transformation of $\hat{c}^\dagger_{k\alpha}$, given by $\hat{\psi}^\dagger_{x\alpha} = \sum_k \frac{e^{-ikx}}{\sqrt{L}}\hat{c}^\dagger_{k\alpha}$, where L is the system size. The time evolution of field operators is defined as $\hat{\psi}^\dagger_{x\alpha}(t) = e^{i\hat{H}_F t}\hat{\psi}^\dagger_{x\alpha}e^{-i\hat{H}_F t}$ for integer t (integer multiples of the period). Utilizing Eq. (S4), we can derive the following expression:

$$\hat{U}(1,0,0)\hat{\psi}^\dagger_{x\alpha}(t)\hat{U}^\dagger(1,0,0) = \hat{\psi}^\dagger_{x'\alpha'}(t'), \tag{S17}$$

where $(t', x')^T = A\,(t, x)^T$, and t, x, t', x' are all integers. The transformation $\hat{U}(1,0,0)$ induces changes in both the spatial and temporal coordinates of the field operators, which are determined by the matrix A.

The propagator of particles in band-α is defined as

$$G_\alpha(t_1x_1, t_2x_2) = -i\theta(t_1 - t_2)\langle\left[\hat{\psi}_{x_1\alpha}(t_1), \hat{\psi}^\dagger_{x_2\alpha}(t_2)\right]_\pm\rangle, \tag{S18}$$

where the plus (minus) sign corresponds to fermions (bosons), and θ represents the Heaviside function. The coordinates t_1, x_1, t_2, x_2 are all integers. The angle brackets $\langle\rangle$ denote the expectation value with respect to the vacuum state. Due to discrete translational symmetry, G_α depends only on the difference $\Delta t = t_1 - t_2$ and $\Delta x = x_1 - x_2$ for integer coordinates. Using Eq. (S17), we immediately find:

$$G_\alpha(\Delta t, \Delta x) = G_{\alpha'}(\Delta t', \Delta x'), \tag{S19}$$

where $(\Delta t', \Delta x')^T = A(\Delta t, \Delta x)^T$. This equation explains how the mixing symmetry manifests in the particle propagator. For $\alpha' = \alpha$ (a singlet band in the $\mathcal{P}_2$ class), the propagator must remain invariant after a linear operation A on the spacetime coordinates, imposing a strong constraint on the propagator. For $\alpha' \neq \alpha$, the propagator of band-α after the coordinate transformation becomes the propagator of band-α'. Thus, Eq. (S19) establishes a connection between propagators of different bands.

In experiments, what can be measured is the wave function, or more precisely, the absolute magnitude of the wave function. The wave function is directly linked to the propagator. If we initially locate a particle at position $x = 0$ at time $t = 0$, its wave function at a later time satisfies, according to Eq. (S18) and (S19),

$$\Psi_\alpha(t, x) = \Psi_{\alpha'}\,(t', x')\,, \tag{S20}$$

where $(t', x')^T = A\,(t, x)^T$ and t, x are arbitrary integers. An alternative way to prove this result is by using $\Psi_\alpha(t, x) = \sum_k e^{ikx - itE_\alpha(k)}/L$ and Eq. (S4).